

## SYNTHESIS AND CHARACTERISATION OF CLOSED CELLS ALUMINIUM FOAMS CONTAINING DOLOMITE POWDER AS FOAMING AGENT

### PRIPRAVA IN KARAKTERIZACIJA ALUMINIJSKIH PEN Z ZAPRTO POROZNOSTJO, IZDELANIH Z DOLOMITNIM PRAHOM KOT SREDSTVOM ZA PENJENJE

Varužan Kevorkijan<sup>1</sup>, Srečo Davor Škapin<sup>2</sup>, Irena Paulin<sup>3</sup>, Borivoj Šuštaršič<sup>3</sup>,  
Monika Jenko<sup>4</sup>

<sup>1</sup>Independent Researcher, Betnavska cesta 6, 2000 Maribor, Slovenia

<sup>2</sup>Institut "Jožef Stefan", Jamova 39, 1000 Ljubljana, Slovenia

<sup>3</sup>Institute of Metals and Technology, Lepi pot 11, 1000 Ljubljana, Slovenia  
varuzan.kevokijan@impol.si

*Prejem rokopisa – received: 2010-07-03; sprejem za objavo – accepted for publication: 2010-08-30*

In this work, the viability of dolomite powder as cost-effective alternative to TiH<sub>2</sub> foaming agent was investigated. Closed cells aluminium foam samples were prepared starts from solid, foamable precursors synthesized by powder metallurgy and melt route. Precursors obtained by melt route were machined and additional cold isostatic pressed in order to improve their density. In all cases, the resulted precursors consisted of an aluminium matrix containing various mass fractions of uniformly dispersed dolomite powders of various average particle size and 5 % of SiC particulates. Precursors were foamed by inserting into a cylindrical stainless steel mould and placing inside a pre-heated batch furnace at 700 °C for 10 min.

The quality of foamable precursors was evaluated by determining their initial density and the foaming efficiency. On the other side, the quality of the obtained foams were characterised by their density, microstructure and mechanical properties.

Experimental findings confirmed that aluminium foams synthesized with dolomite powder as blowing agent can be prepared by both powder metallurgy and melt route, as well as that the density, microstructure, compression strength, and energy absorption capacity are quite comparable with corresponding counterparts foamed by TiH<sub>2</sub>.

Key words: closed cells aluminium foams, dolomite particles as foaming agent, powder metallurgy, melt route, foaming efficiency, mechanical properties

V delu preučujemo možnost nadomeščanja TiH<sub>2</sub> kot sredstva za penjenje z dolomitnim prahom. Vzorci aluminijske pene smo pripravili s prekurzorji, izdelanimi po postopku metalurgije prahov in po livarskem postopku. Prekurzorje, izdelane po livarskem postopku, smo tudi strojno obdelali in nato še hladno izostatsko stisnili, da smo povečali njihovo gostoto. Ne glede na postopek njihove izdelave, so dobljeni prekurzorji vsebovali aluminijsko matriko in v njej različne koncentracije enakomerno porazdeljenih delcev dolomita ter SiC-delcev različnih povprečnih velikosti. Pene smo v nadaljevanju izdelovali tako, da smo prekurzor zaprli v za ta namen izdelan jekleni model, ki smo ga nato za 10 min vstavljali v peč, ogreto na 700 °C.

Kakovost prekurzorjev za penjenje smo ugotavljali na osnovi njihove gostote in učinkovitosti penjenja. Po drugi strani smo kakovost izdelanih pen določali na osnovi njihove gostote, mikrostrukture in mehanskih lastnosti.

Eksploimentalne ugotovitve so potrdile, da je aluminijske pene mogoče izdelovati z dolomitnim prahom kot sredstvom za penjenje, tako po postopku prašne metalurgije kakor tudi po livarskem postopku in tako, da so njihova gostota, mikrostruktura, tlačna trdnost in sposobnost absorpcije energije povsem primerljive z vrednostmi, ki jih navaja literatura za Al-pene, izdelane s TiH<sub>2</sub>-penilom.

Ključne besede: aluminijske pene z zaprto poroznostjo, delci dolomita kot sredstva za penjenje, postopki metalurgije prahov, livarski postopki, učinkovitost penjenja, mehanske lastnosti

## 1 INTRODUCTION

Since last few decades, closed cells aluminium foams – one of the lightest engineered materials have been subject of investigation<sup>1,2</sup> as candidate for a broad range of applications. However, instead of significant progress made in aluminium foams manufacturing, as well as properties development and optimisation, a longed expected commercialisation of this class of materials remained poor. The limited commercial potential of aluminium foams is mostly affected by its inadequate viability (the insufficient balance between its technical and economical attributes) caused by high cost and

properties which are not always in line with customers expectations.

Closed cells aluminium foams are produced either by (i) direct foaming methods starting from slurry of molten aluminium or aluminium alloys and uniformly dispersed non-metallic particles to which gas bubbles are added to create foam, and (ii) indirect foaming methods starting from a solid, foamable precursor which upon melting expands and transforms to foam.<sup>3</sup> The foamable precursor, aluminium-based matrix containing uniformly dispersed blowing agent particles, can be produced either by powder metallurgy<sup>4</sup> or melt route.<sup>5</sup>

The direct foaming methods are cost-effectively but result only in medium quality level of foams. On the

other side, the closed cells aluminium foams produced by indirect foaming of precursors made by powder metallurgy route are with the superior quality but, at the same time, very high cost. Precursors made by melt route are with significantly lower cost, replacing the expensive aluminium powder by conventional melt. The additional reducing of cost can be achieved by replacing expensive  $TiH_2$  with alternative inexpensive blowing agents, particularly carbonates such as  $CaCO_3$ . The  $CaCO_3$  was applied for successful indirect preparation of aluminium foams by powder metallurgy and melt route.<sup>6</sup> The usage of other carbonates (e.g.  $MgCO_3$  and  $CaMg(CO_3)_2$ ) was also reported but not as often as  $CaCO_3$ .

Among its significantly lower cost compared to the cost of  $TiH_2$ ,  $CaCO_3$  as the blowing agent has also several other advantages. As detailed discussed by Gergely et al.,<sup>5</sup>  $CaCO_3$  reacts with molten aluminium creating the foaming gas ( $CO_2$ ) and various solid particles, depending on the composition of the aluminium alloy ( $CaO$ ,  $Al_2O_3$ ,  $Al_4C_3$  and  $MgAl_2O_4$ ). In contrast to  $TiH_2$  which decomposition leads to the formation of chemically inert hydrogen, the  $CO_2$  foaming gas obtained by the decomposition of  $CaCO_3$  reacts with melt stabilising the foam suspension. The results of Gergely et al.<sup>5</sup> suggest that, as a result of foaming gas ( $CO_2$ )/melt reaction, a thin solid reaction layer forms in the early stages of the foaming process stabilising, by the beneficial effect on the surface tension modification, the cells against coarsening and coalescence. In addition, the solid particles obtained by thermal decomposition of  $CaCO_3$  enhance the melt viscosity, further promoting the stabilisation of the foam.

On the other side, the main disadvantage of  $CaCO_3$  as foaming agent is its relatively high decomposition temperature (between 700 °C and 900 °C) – significantly above the melting point of pure aluminium and aluminium alloys. High foaming temperature makes aluminium foams stabilisation more demanding and costly. However, an opposite problem exists with  $TiH_2$ . It decomposes far below the melting point of aluminium and aluminium alloys and thereof should be surface engineered<sup>8</sup> in order to shift the decomposition temperature closed to the melting point of aluminium alloys, which introduces additional cost.

One of the most important steps in production of aluminium foams is their stabilisation. Either in direct or indirect methods, foaming is always initiated by dispersing a large number of gas bubbles into a melt, leading to the formation of stable slurry. The solid foam is then fabricated by freezing the obtained slurry through solidification process. Thereof, during processing aluminium foam is going through a series of transient states which changes its morphology considerably. Generally, foams are kinetically stable, if do not change significantly in the time span between completion of the blowing process and solidification. Although aluminium foam stabilisation has been well discussed in literature and numerous models of foam stability were presented,<sup>3</sup> the

reason for their stability in the liquid or semi-liquid state is still under dispute. However, it has been shown that aluminium melts without a solid phase are not foamable. Furthermore, it has been demonstrated that the stable slurry of gas bubbles in molten metal is an important prerequisite for obtaining more uniform microstructure of the end product, without irregularities caused by coarsening and coalescence. The effect of various processing parameters (temperature, time, melt viscosity, surface tension, wetting behaviour etc.) on the foamability of aluminium alloys and stability of slurry of gas bubbles in molten metal has been also investigated.<sup>4,9–11</sup> It was found that aluminium foam slurry stabilisation is the most effective at temperatures slightly below or above the melting point of Al or the applied Al alloy. The processing time should be properly controlled due to the fact that the pore size and the total porosity volume increase with time. Thereof, very short processing time will result in fine pores but also the low total porosity and low energy absorption capacity. The existence of the solid particles in the melt is necessary for nucleation of bubbles and the increase in viscosity. Viscosity is one of the most important parameters influencing the foam stability and should be kept inside the proper processing window. An increase of viscosity generally enhances the stability of the bubbles in slurry but also influences their size and foam microstructure development. Finally, lowering of the surface tension of the molten metal (e.g. addition of magnesium) and improving wetting of solid particles with melt significantly was found to enhance significantly stabilisation of gas bubbles inside the slurry.

Although the development of aluminium foams looks back on a long history, none of the processes available nowadays has been sophisticated to a level comparable with that of polymeric foams. The reasons for that are lack of understanding of the basic mechanism of aluminium foaming, insufficient ability to make Al foams of a constant quality, knowledge of aluminium foam properties is insufficient, physical properties of Al foams are not good enough, transfer of research results to design engineers is insufficient and Al foams are still too expensive.<sup>3</sup>

Further improving of the competitiveness of the indirect foaming of aluminium alloys it is particularly important to formulate the cost-effective blowing agent which thermal decomposition will proceed (would happen) at temperature close to the melting point of the selected alloy, evolving at the same time gaseous and solid products well involved in stabilisation of foamed slurry.

Considering that aluminium foam slurry stabilisation is most effective at temperatures slightly below or above the melting point of Al or the selected Al alloy, the most suitable blowing agent should decomposes mostly inside that temperature interval. Stabilisation of foam slurries at

temperatures far below or above the temperature of liquidus is more difficult and costly.

In the present paper, the performance of dolomite powder as a cost-effective foaming agent was investigated in both powder metallurgy and melt route of foams preparation. The influence of various processing parameters on foaming behaviour, as well as the development of foam microstructure and mechanical properties was also discussed.

## 2 EXPERIMENTAL PROCEDURE

All foams made in this work were prepared by indirect foaming methods starts from a solid, foamable precursor which consists of a metallic matrix containing uniformly dispersed blowing agent particles. Foamable precursors were made by: (i) powder metallurgy route and (ii) melt route by using the same blowing agent – dolomite powders (type A, B and C) with various average particle sizes ((44, 76 and 97)  $\mu\text{m}$ , respectively).

The morphology of as received dolomite powders was investigated by scanning electron microscopy (SEM/EDS) whereas X-ray diffraction (XRD) measurements were applied to identify the phases and their crystal structure. In addition, the thermogravimetric analysis (TGA) was also performed in a Setaram Labsys DTA1600 equipment.

By following the powder metallurgy (P/M) route, foamable precursors were made by mixing Al powder, with an average particle size of 63  $\mu\text{m}$  (purity: 99.7 %, oxygen content: 0.25 %), 5 % of SiC particles with an average particle size of 10  $\mu\text{m}$  and (3, 5, 7 and 12) % of blowing agent, followed by cold compaction, in a lubricated 20 mm diameter die, to a pressure of 600MPa to 900MPa.

In the case of melt route, foamable precursors with the same concentration of dolomite blowing agent ((3, 5, 7 and 12) %) and the same geometry are prepared by a induction heated batch-type stir-casted in which aluminium powder (the same used for the P/M route) was induction melted, followed by the addition of dolomite particles, stirring and casting. Once molten aluminium heated to 700 °C, the power addition was switched off and melt stirring was initiated until the temperature of melt decreased to 685 °C. After that, the blowing agent/aluminium powder mixture (1 : 2 mass ratio) was introduced and the melt was stirred (at approximately 1200 r/min) for additional 30-90 s. Finally, foamable precursors were prepared by casting the semi-solid slurry into a room temperature mould with 20 mm diameter.

The solidified precursors were machined and some of samples were additionally cold isostatically pressed.

The density of foamable precursors was calculated from the mass and geometry of the samples and, in addition, measured by Archimedes method. The distribution of blowing agent particulates inside Al matrix was

examined by analysing the optical and scanning electron micrographs of as polished bars.

All precursors were foamed in a conventional batch furnace with air atmosphere circulation under the same experimental conditions (temperature, time, cooling method). Before foaming, the individual precursors were inserted into a cylindrical (40 mm in diameter, 70 mm long) stainless steel mould coated with a boron nitride suspension. The mould dimensions and the precursor size (20 mm in diameter and 60 mm long) were selected to allow an expansion of the precursor to foam with theoretical density closed to 0.6 g/cm<sup>3</sup>. The arrangement was placed inside a pre-heated batch furnace at 700 °C for 10 min. After that period of time, the mould was removed from the furnace and the foaming process was stopped by rapid cooling with pressurised air to room temperature. The thermal history of the foam sample was recorded, using a thermocouple located directly in the precursor material.

Foam density using the Archimedes method was carried out. The porosity of manufactured foam was calculated by the rate: 1-(foam density/aluminium density). Macro and microstructural examination was performed on sectioned obtained by wire precision cutting across the samples and on samples mounted in epoxy resin, using optical and scanning electron microscopy (SEM/EDS).

An average particle size of pores in the foams was estimated by analysing the optical and scanning electron micrographs of as polished foam bars using the point counting method and image analysis and processing software.

Regarding mechanical properties of the foams, the uniaxial room temperature compressive tests were carried out on a Instron 1255 testing machine at a constant 5 mm/min crosshead displacement. Testing was performed on standard prismatic foam specimens of 50 mm x 12 mm x 17 mm so that each point of the stress-strain curve was determined as an average of four individual measurements. Compression was stopped whenever either 80 % strain or 95 kN force (equivalent to 61.9 MPa) were reached. As a result of testing, the uniaxial compression stress-strain curve, compressive strength and energy absorption after a 30 % strain were determined and correlated with the density, the average pore size and microstructure of foam samples.

## 3 RESULTS AND DISCUSSION

### 3.1 Morphology investigation of performs and aluminium foams

Morphology of the applied foaming agent – dolomite powder grade A is presented in **Figure 1**. As evident, dolomite particles are irregularly shaped and non-agglomerated.

XRD analysis of dolomite powder (grade A) revealed the presence of about 5 % of calcium carbonate as an

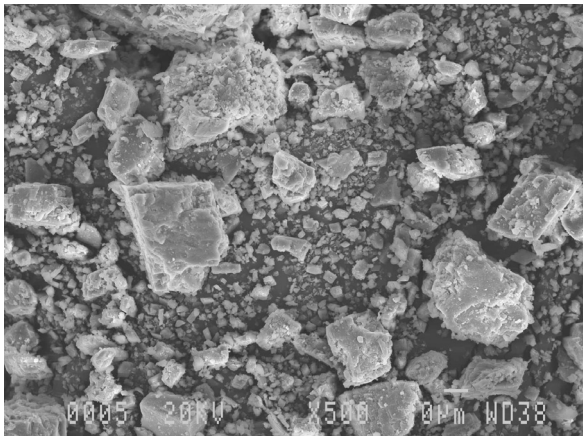


**Figure 1:** SEM micrograph showing the size and morphology of the foaming agent – dolomite powder grade A.

**Slika 1:** SEM-posnetek dolomitnega prahu (tip A)

impurity, **Figure 2**. Thereof, the foaming agent (as received dolomite powder) consisted of 95 % of dolomite and 5 % of  $\text{CaCO}_3$ .

Thermogravimetric (TGA) curve for the dolomite powder is plotted in **Figure 3**. TGA analysis has shown that dolomite powder undergoes thermal decomposition above approximately 650 °C and that decomposition ends about 830 °C. Because of that, higher foaming temperatures are necessary than with  $\text{TiH}_2$  precursor, particularly when higher foaming efficiency on final foams is required. On the other side, higher onset temperature of  $\text{CO}_2$  evolution from dolomite powder enabling the incorporation of dolomite particles into aluminium melt without the need of any special pre-treatment in order to prevent premature gas-release. Separate TGA measurement (not present here) showed that the kinetics of gas-release (dolomite mass loss) are slightly slower in the case of larger dolomite particulates.

Microstructures of cold isostatically pressed performs obtained by powder metallurgy and melt route were also analysed by SEM; **Figures 4 and 5**.

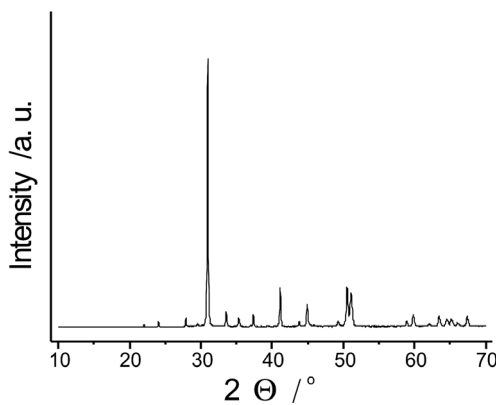


**Figure 2:** XRD of dolomite powder (grade A) showing the presence of approx. 5 % of  $\text{CaCO}_3$  phase

**Slika 2:** XRD vzorca dolomitnega prahu (tip A), ki potrjuje prisotnost pribl. 5 %  $\text{CaCO}_3$ -faze

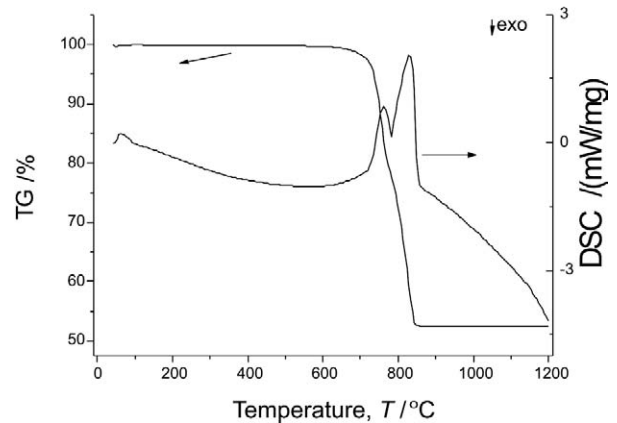


**Figure 3:** Thermogravimetric (TG) and differential scanning calorimetric (DSC) measurement curves for dolomite powder grade A.

**Slika 3:** TGA dolomitnega prahu (tip A)

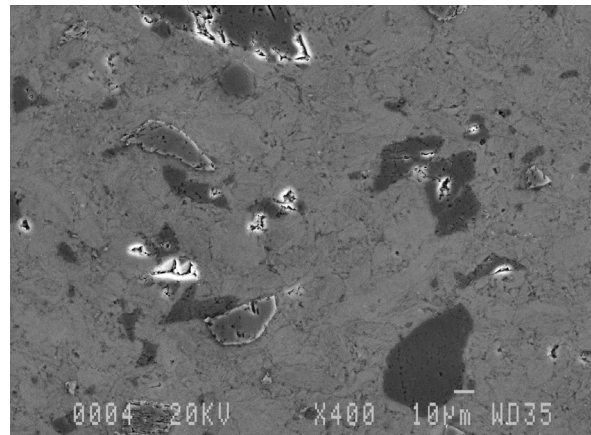


**Figure 4:** SEM micrograph of cold isostatically pressed preform obtained by powder metallurgical route reveals almost fully dense aluminium matrix, dolomite (dark) and silicon carbide (gray) particles without particles agglomeration or particle fracture

**Slika 4:** SEM-posnetek hladno izostatsko stisnjene prekurzorja, izdelanega po postopku prašne metalurgije, ki razkriva gosto sintrano aluminjsko matriko ter neaglomerirane delce dolomita (temno) in silicijevega karbida (sivo)

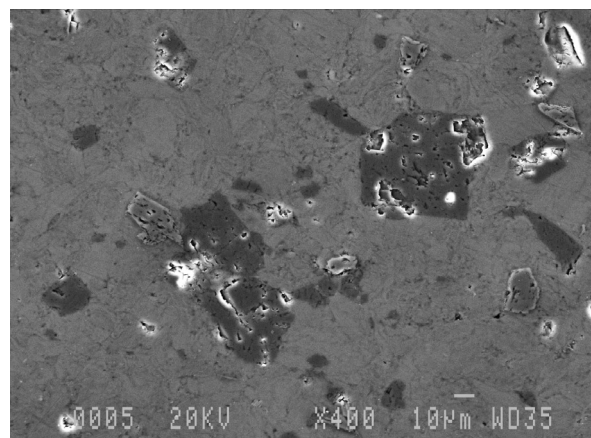


**Figure 5:** SEM micrograph of cold isostatically pressed preform obtained by melt route

**Slika 5:** SEM-posnetek hladno izostatsko stisnjene prekurzorja, izdelanega po livarskem postopku

The measured and calculated densities of foamable performs obtained by P/M route, **Table 1**, confirmed that under the applied pressure of isostatic pressing (740 MPa) all performs were with closed porosity and densities above 98 % of theoretical. However, a density >99 % of theoretical was achieved for precursors containing 3–7 % of dolomite particles, with higher addition this could not be achieved resulting in lower foaming efficiency, as evident in **Table 4**. The foaming efficiency of preforms was evaluated based on the relative density of the obtained foam  $\rho_r$ , calculated by dividing the apparent density of the foam  $\rho_F$ , with the density of the aluminium,  $\rho_{Al}$ . Thereof, the foaming efficiency is expressed as:

$$\eta = 1 - \rho_r = 1 - (\rho_F/\rho_{Al}) \quad (1)$$

which actually corresponds to the volume fraction of pores in foam samples. Lower the foam density, higher is foaming efficiency.

Densities of as-machined foamable performs obtained by melt route were significantly lower compared to PM counterparts, **Table 2**. Moreover, in performs prepared by melt route most of porosity was opened, causing during foaming lower foaming efficiency, as documented in **Table 5**. However, by additional isostatic pressing, the remaining porosity in performs fabricated by melt route was efficiently reduced below the volume fraction 1.2 %, **Table 3**, enabling the formation of aluminium foams with improved foaming performances, **Table 6**.

In all cases, experimental results clearly indicate that the porosity measured in foamable performs and the apparent density achieved in aluminium foam samples are inversely proportioned. Generally, foamable performs with lower porosity resulted in foam samples with higher apparent density and lower foaming efficiency.

**Table 1:** Porosity of foamable performs obtained by PM route

**Tabela 1:** Poroznost prekurzorjev izdelanih s postopkom prašne metalurgije

Chemical composition of performs w/%			Porosity ρ/%	
Dolomite	SiC	Al powder	Calculated	Measured
Type-A				
3	5	92	0.7 ± 0.07	0.7 ± 0.04
5	5	90	0.8 ± 0.08	0.8 ± 0.04
7	5	88	0.9 ± 0.09	1.0 ± 0.05
10	5	85	1.2 ± 0.12	1.3 ± 0.07
Type-B				
3	5	92	1.0 ± 0.10	1.0 ± 0.05
5	5	90	1.0 ± 0.10	1.1 ± 0.06
7	5	88	1.2 ± 0.12	1.3 ± 0.07
10	5	85	1.6 ± 0.16	1.8 ± 0.09
Type-C				
3	5	92	1.1 ± 0.11	1.1 ± 0.06
5	5	90	1.2 ± 0.12	1.3 ± 0.06
7	5	88	1.3 ± 0.13	1.4 ± 0.07
10	5	85	1.8 ± 0.18	2.0 ± 0.10

**Table 2:** Porosity of as-machined foamable performs prepared by melt route

**Tabela 2:** Poroznost strojno obdelanih prekurzorjev, izdelanih po livarskem postopku.

Chemical composition of performs w/%			Porosity ρ/%	
Dolomite	SiC	Al powder	Calculated	Measured
Type-A				
3	5	92	4.7 ± 0.47	4.9 ± 0.25
5	5	90	4.9 ± 0.49	5.1 ± 0.26
7	5	88	5.4 ± 0.54	5.8 ± 0.29
10	5	85	6.1 ± 0.61	6.6 ± 0.33
Type-B				
3	5	92	4.5 ± 0.45	4.7 ± 0.24
5	5	90	4.7 ± 0.47	5.0 ± 0.25
7	5	88	5.0 ± 0.50	5.3 ± 0.27
10	5	85	5.7 ± 0.57	6.2 ± 0.31
Type-C				
3	5	92	4.4 ± 0.44	4.5 ± 0.23
5	5	90	4.5 ± 0.45	4.7 ± 0.24
7	5	88	4.7 ± 0.47	5.0 ± 0.25
10	5	85	4.9 ± 0.49	5.3 ± 0.27

**Table 3:** Porosity of foamable performs obtained by melt route improved by the additional isostatic pressing

**Tabela 3:** Poroznost prekurzorjev, izdelanih po livarskem postopku, izboljšana z dodatnim hladnim izostatskim stiskanjem

Chemical composition of performs w/%			Porosity ρ/%	
Dolomite	SiC	Al powder	Calculated	Measured
Type-A				
3	5	92	0.9 ± 0.09	0.9 ± 0.05
5	5	90	0.9 ± 0.09	0.9 ± 0.05
7	5	88	1.0 ± 0.10	1.1 ± 0.06
10	5	85	1.1 ± 0.11	1.2 ± 0.06
Type-B				
3	5	92	0.9 ± 0.09	0.9 ± 0.05
5	5	90	0.9 ± 0.09	0.9 ± 0.05
7	5	88	0.9 ± 0.09	1.0 ± 0.05
10	5	85	1.0 ± 0.10	1.1 ± 0.06
Type-C				
3	5	92	0.8 ± 0.08	0.8 ± 0.04
5	5	90	0.8 ± 0.08	0.8 ± 0.04
7	5	88	0.8 ± 0.08	0.9 ± 0.05
10	5	85	0.9 ± 0.09	1.0 ± 0.05

**Table 4:** Density, foaming efficiency and the average pore size of aluminium foams prepared by PM route

**Tabela 4:** Gostota, učinkovitost penjenja in povprečna velikost por v aluminijških penah, izdelanih po postopku prašne metalurgije

Initial composition of foamable performs w/%			Selected properties of foamed samples		
Dolomite	SiC	Al powder	Density (g/cm <sup>3</sup> )	Foaming efficiency (%)	Average pore size (mm)
Type-A					
3	5	92	0.56 ± 0.03	79,3	0.9 ± 0.09
5	5	90	0.59 ± 0.03	78,1	0.9 ± 0.09
7	5	88	0.63 ± 0.03	76,7	1.1 ± 0.11

10	5	85	0.69 ± 0.03	74,4	1.3 ± 0.13
Type-B					
3	5	92	0.51 ± 0.03	81,1	0.6 ± 0.06
5	5	90	0.53 ± 0.03	80,4	0.7 ± 0.07
7	5	88	0.57 ± 0.03	78,9	0.9 ± 0.09
10	5	85	0.59 ± 0.03	78,1	0.9 ± 0.09
Type-C					
3	5	92	0.50 ± 0.03	81,5	0.6 ± 0.06
5	5	90	0.52 ± 0.03	80,7	0.6 ± 0.06
7	5	88	0.55 ± 0.03	79,6	0.8 ± 0.08
10	5	85	0.56 ± 0.03	79,3	0.9 ± 0.09

**Table 5:** Density, foaming efficiency and the average pore size of aluminium foams prepared from as-machined foamable performs fabricated by melt route

**Tabela 5:** Gostota, učinkovitost penjenja in povprečna velikost por v aluminijških penah, izdelanih iz strojno obdelanih prekurzorjev, dobljenih po livarskem postopku

Initial composition of foamable performs w/%			Selected properties of foamed samples		
Dolomite	SiC	Al powder	Density (g/cm <sup>3</sup> )	Foaming efficiency (%)	Average pore size (mm)
Type-A					
3	5	92	0.71 ± 0.04	73,7	1.2 ± 0.12
5	5	90	0.72 ± 0.04	73,3	1.4 ± 0.14
7	5	88	0.75 ± 0.04	72,2	1.4 ± 0.14
10	5	85	0.81 ± 0.04	70,0	1.5 ± 0.15
Type-B					
3	5	92	0.61 ± 0.03	77,4	0.8 ± 0.08
5	5	90	0.63 ± 0.03	76,6	0.9 ± 0.09
7	5	88	0.66 ± 0.03	75,5	1.0 ± 0.10
10	5	85	0.70 ± 0.04	74,1	1.1 ± 0.11
Type-C					
3	5	92	0.65 ± 0.03	75,9	0.8 ± 0.08
5	5	90	0.66 ± 0.03	75,5	0.9 ± 0.09
7	5	88	0.68 ± 0.03	74,8	1.1 ± 0.11
10	5	85	0.72 ± 0.04	73,3	1.5 ± 0.15

**Table 6:** Density, foaming efficiency and the average pore size of aluminium foams prepared by melt route from as-machined and additionally isostatically pressed foamable performs

**Tabela 6:** Gostota, učinkovitost penjenja in povprečna velikost por v aluminijških penah, izdelanih iz strojno obdelanih in hladno izostatsko stisnjenih prekurzorjev, dobljenih po livarskem postopku

Initial composition of foamable performs w/%			Selected properties of foamed samples		
Dolomite	SiC	Al powder	Density (g/cm <sup>3</sup> )	Foaming efficiency (%)	Average pore size (mm)
Type-A					
3	5	92	0.63 ± 0.03	76,7	1.1 ± 0.11
5	5	90	0.67 ± 0.03	75,2	1.2 ± 0.12
7	5	88	0.71 ± 0.03	73,7	1.3 ± 0.13
10	5	85	0.78 ± 0.03	71,1	1.6 ± 0.16
Type-B					
3	5	92	0.57 ± 0.03	78,9	0.7 ± 0.07
5	5	90	0.59 ± 0.03	78,1	0.9 ± 0.09
7	5	88	0.62 ± 0.03	77,0	1.1 ± 0.11
10	5	85	0.63 ± 0.03	76,7	1.4 ± 0.14

Type-C					
3	5	92	0.58 ± 0.03	78,5	0.7 ± 0.07
5	5	90	0.60 ± 0.03	77,8	0.8 ± 0.08
7	5	88	0.64 ± 0.03	76,3	1.0 ± 0.10
10	5	85	0.67 ± 0.03	75,2	1.1 ± 0.11

### 3.2 Microstructure investigation of aluminium foam samples

The similar cellular structure development with spherical, closed pores was obtained by both powder metallurgy, **Figure 6**, and melt processing route, **Figure 7**. However, as evident in **Figure 6**, the samples obtained by powder metallurgy route were with more uniform microstructure consisted of well separated individual cells. On the other hand, the microstructure of samples obtained by melt processing route, **Figure 7**, revealed the presence of non-uniformities caused by insufficient

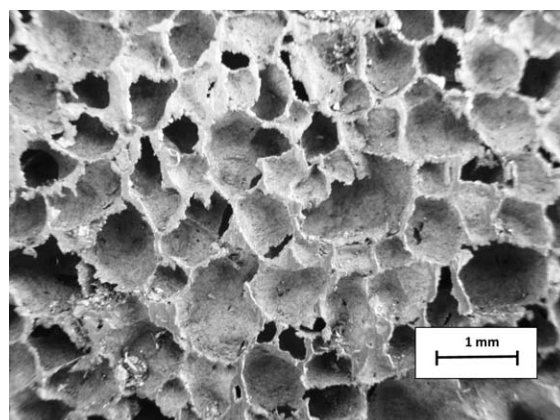


**Figure 6:** Cross section of aluminium foams obtained by P/M route with well separated individual cells and relatively uniform microstructure

**Slika 6:** Posnetek prečnega prereza vzorca aluminijške pene, izdelane po postopku prašne metalurgije, z izraženimi posameznimi porami in relativno enakomerno mikrostrukturo

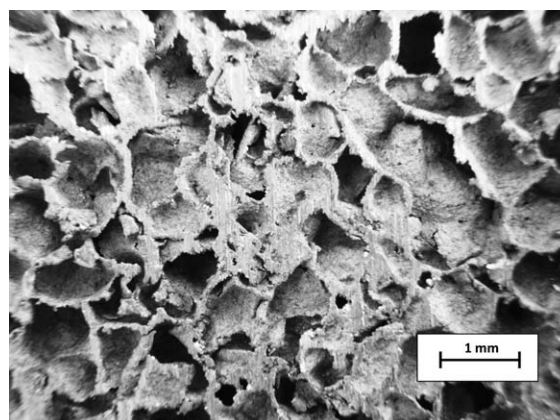


**Figure 7:** Cross section of aluminium foam obtained by melting route with characteristic channel network and foam drainage

**Slika 7:** Posnetek prečnega prereza vzorca aluminijške pene, izdelane po livarskem postopku, na katerem so poleg posameznih por opazne tudi nehomogenosti, povzročene z zlitjem por in odtokanjem taline skozi značilne kanale v mikrostrukturi

stability of foams in transient states of their formation. The most of observed imperfections were created by flow (the movement of bubbles with respect to each other), drainage (flow of liquid metal through the intersection of three foam films), coalescence (sudden instability in a foam film) and coarsening (slow diffusion of gas from smaller bubbles to larger ones).

The absence of pore coarsening and drainage suggests that there is a cell face stabilising mechanism operating in the carbonate-foamed melts,<sup>5</sup> slowing down the cell face rupturing process and hence inhibiting cell coarsening. The mechanism is likely to be a result of the foaming gas (CO<sub>2</sub>)/melt or semi solid slurry reaction during the foaming procedure which was detailed discussed by Gergely et al.<sup>5</sup>

Concerning the average pore size and the uniformity in cell size distribution, foams made by P/M route are with finer pores and more regular morphology than samples made by melt route, particularly these from as-machined precursors. However, an additional cold isostatically pressing of as-machined precursor obtained by melt route was found to help in achieving more uniform foams with smaller average pore size similar to that obtained by P/M route. The improvement is most probably caused by better compacting of individual dolomite particles and aluminium matrix, resulting in higher density of foamable precursor.

### 3.3 Mechanical properties

**Figure 8** shows an example of stress-strain response of samples foamed from performs prepared by P/M in which the compressive strength of the foams was correlated with their density.

Because of the closed cells structure, compressive foam behaviour showed in all cases the typical stress-strain diagram with a division on three parts: a linear

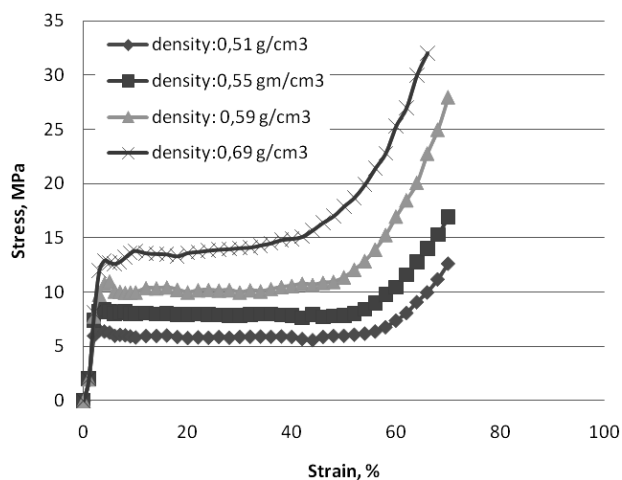


**Figure 8:** The stress-strain response of various aluminium foam samples from performs obtained by PM

**Slika 8:** Krivulja napetost – deformacija za vzorce aluminijških pen na osnovi predoblik, izdelanih po postopku prašne metalurgije

increase in strength mainly caused by elastic deformation, followed by a plateau caused by homogeneous plastic deformation and a final step increase due to the collapse of the cells. The compressive strength was taken as the initial peak stress. Foams made by PM route become with highest compressive strength, while samples foamed from as-machined precursors were with significantly lower values. For interval of foam densities analysed in this work (from 0.5 g/cm<sup>3</sup> to 0.7 g/cm<sup>3</sup>), it was found that more dense foam samples shifted the position of the plateau toward higher stress values.

The energy absorbed per unit volume (*E*-energy absorption capacity), which is one of the most important characteristic of aluminium foams, was determined by the area under the stress-strain plots as follows:<sup>12</sup>

$$E = \int_0^l \sigma(\epsilon) d\epsilon \quad (2)$$

where  $\sigma$  is compressive stress,  $l$  is the limit of strain concerned and  $\epsilon$  is compressive strain. The calculated values of energy absorption capacity for samples were plotted in **Figure 9** and correlated with foams density. The typical response was found to be a quasi-Gaussian function with a maximum energy absorption capacity at very narrow density range.

The maximum energy absorption capacity for various foams is summarized in **Figure 9**. For foams made by P/M route, the maximum energy absorption capacity of 6.82 MJ/m<sup>3</sup> is achieved in foams with density of 0.63 g/cm<sup>3</sup>. On the other side, in samples foamed from as-machined precursors fabricated by melt route, maximum energy absorption capacity of only 5.42 MJ/m<sup>3</sup> was detected. The maximum appeared at foam density of 0.65 g/cm<sup>3</sup>. Finally, in melt route fabricated precursors additionally isostatically pressed before foaming, an

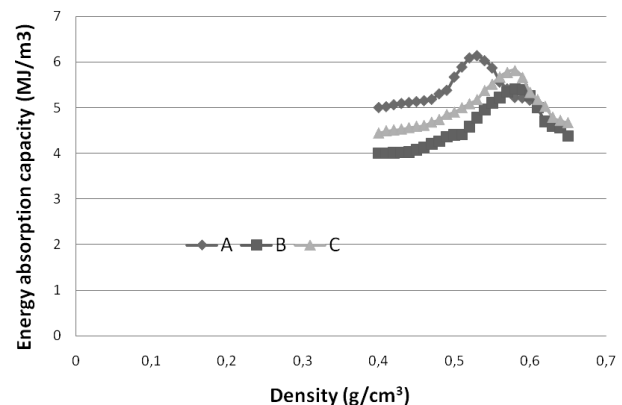


**Figure 9:** Example of the optimization of aluminium foam density range for maximum energy absorption capacity: A) foams obtained by powder metallurgy, B) foams obtained from as-machined precursors fabricated by melting route, and C) foams obtained from as-machined and cold isostatically pressed precursors fabricated by melting route

**Slika 9:** Primer optimiziranja gostote vzorcev aluminijških pen za doseganje največje sposobnosti absorpcije energije: A) pene, izdelane po postopku prašne metalurgije; B) pene iz strojno obdelanih prekurzorjev, narejenih po livarskem postopku; C) pene iz strojno obdelanih in hladno izostatsko stisnjenih prekurzorjev, narejenih po livarskem postopku

intermediate maximum energy absorption capacity of  $6.23 \text{ MJ/m}^3$  was detected in samples with density of  $0.63 \text{ g/cm}^3$ .

The foaming process principally does not affect the properties of the cell-wall material. However, it leads to a unique spatial distribution of aluminium which results in significantly different properties of foamed component in comparison with a bulk part. It is obvious that the properties of aluminium foam significantly depend on its porosity, so that a desired property (or combination of properties) can be tailored by selecting the foam density.

The mechanical properties of foams obtained by applying dolomite powder as foaming agent are fully comparable with counterpart properties in foams fabricated by using  $\text{TiH}_2$ .

#### 4 CONCLUSION

The following conclusions can be drawn from this work.

$\text{TiH}_2$  powder as foaming agent was successfully replaced by commercial dolomite powders of different average particle size, fabricated by milling of nature mineral.

Foaming precursors with different volume portions (3–10 %) of dolomite powder particles as blowing agent were routinely prepared neither by powder metallurgy or melt route. Precursors obtained by powder metallurgy were with superior homogeneity and densities above 98 % of theoretical. The counterparts obtained by melt route were with more agglomerated dolomite particles and significantly lower densities ( $\geq 93.4$  % of theoretical). However, it was found that an additional cold isostatic pressing of these precursors improved their densities up to 97.4 % of theoretical.

Density above 99 % of theoretical was achieved only for precursors obtained by PM and melt route (improved by additional isostatic pressing), containing 3–7 % of dolomite particles of an average particle size of  $44 \mu\text{m}$ . With higher addition of dolomite particles and by using dolomite powders with higher average particle size ( $76 \mu\text{m}$  and  $97 \mu\text{m}$ ) densities  $\geq 99$  % of theoretical could not be achieved.

The foaming efficiency of experimentally prepared precursors was evaluated based on the relative density of the obtained foams (the apparent density of the foam divided by the density of aluminium). The experimental findings shown that the apparent density of foam samples is inversely proportional to the density of foaming precursor. Thereof, foamable precursors with higher density resulted in foam samples with lower apparent density and higher foaming efficiency. Foaming of almost fully dense precursors (densified above 99 % of theoretical density) resulted in foam samples with the lowest densities (typically from  $0.50 \text{ g/cm}^3$  to  $0.6 \text{ g/cm}^3$ ) and hence high foaming efficiency ( $\geq 75$  %). In opposite, foaming of precursors densified below 97 % of theoret-

ical led to foams with higher densities (from  $0.7 \text{ g/cm}^3$  to  $0.8 \text{ g/cm}^3$ ) and lower foaming efficiency (below 75 %).

Under the same foaming conditions (temperature, time), the average pore size of foam samples is influenced by the density of the foaming precursors and the initial size of the foaming particles. As a rule, in foams made from precursors with high density ( $\geq 99$  % of theoretical), the average pore size remained below 1 mm. On the other side, in foams made from precursors with lower density (below 97 % of theoretical), pores grown to 20 % to 50 % higher average pore size. Regarding the initial size of the foaming particles, which also influences the density of precursor and hence the density of the foam samples, an increase of the average particle size of dolomite foaming agent was observed to have the detrimental influence on the average size of pores. Coarser dolomite powders led to the formation of larger bubbles in foam structure. By introducing the term of foaming efficiency, which in simple and transparent way includes all experimental influences, it was possible to establish the direct correlation between the foaming efficiency and the average pore size as one of the main parameters of the microstructure of foamed samples. The experimental findings confirmed that the foaming efficiency and the average pore size of foaming samples are generally reciprocally depended. Thereof, higher foaming efficiency results in foam microstructure with finer pores.

Mechanical properties (compression strength and energy absorption capacity) of foamed samples are also strongly influenced by foaming efficiency. For interval of foam densities analysed, the compression strength, considered as the initial peak stress, was found to be superior (approx. 13.8 MPa) in samples with increased density ( $0.69 \text{ g/cm}^3$ ) and thereof lower foaming efficiency (74.4 %). In opposite to that, the maximum energy absorption capacity was achieved in foams with the highest foaming efficiency. The stress-strain response of foamed samples consisted of three parts: a linear increase in strength mainly caused by elastic deformation, followed by a plateau caused by homogeneous plastic deformation and a final step increase due to the collapse of the cells. On the contrary, the energy absorption capacity is a quasi-Gaussian function of density, approaching maximum absorption capacity at very narrow density range.

From experimental findings is obvious that the properties of aluminium foam significantly depend on its porosity, so that a desired property (or combination of properties) can be tailored by selecting the foam density.

Foams synthesized with dolomite powder particles as blowing agent can be cost effectively prepared by both powder metallurgy and melt route. However, the decomposition characteristics of dolomite powder enabling the foaming of aluminium and aluminium alloys only above its melting point.

Experimental findings confirm that microstructure, compression strength and energy absorption capacity of aluminium foams prepared by dolomite powder as foaming agent are quite comparable with these in counterparts foamed by TiH<sub>2</sub>.

## 5 REFERENCES

- <sup>1</sup> J. Banhart, *Int. J. Vehicle Design*, 37 (2005) 2/3, 114
- <sup>2</sup> E. M. A. Maine, M. F. Ashby, *Mater Design*, 23 (2002) 3, 307
- <sup>3</sup> J. Banhart, *Adv. Eng. Mater.*, 8 (2006) 9, 781
- <sup>4</sup> S. Asavavisithchai, A. R. Kennedy, *Scripta Mater.*, 54 (2006), 1331
- <sup>5</sup> V. Gergely, D. C. Curra, T. W. Clyne, *Composites Science and Technology*, 63 (2003), 2301
- <sup>6</sup> L. E. G. Cambroner, J. M. Ruiz-Roman, F. A. Corpas, J. M. Ruiz Prieto, *Journal of Materials Processing Technology*, 209 (2009), 1803
- <sup>7</sup> US Pat. No. 7.452.402, issued November 18, 2008
- <sup>8</sup> B. Matijasevic, J. Banhart, *Scripta Mater.*, 54 (2006), 503
- <sup>9</sup> G. Kaptay, *Colloids and Surfaces A: Physicochemi. Eng. Aspects*, 230 (2004), 67
- <sup>10</sup> V. C. Srivastava, K. L. Sahoo, *Materials Science – Poland*, 25 (2007) 3, 733
- <sup>11</sup> C. C. Yang, H. Nakae, *Journal of Materials Processing Technology*, 141 (2003) 202
- <sup>12</sup> S. Asavavisithchai, R. Tantisiriphaiboon, *Chiang Mai J. Sci.*, 36 (2009) 3, 302

## Acknowledgement

This work was supported by funding from the Public Agency for Research and Development of the Republic of Slovenia, as well as the Impol Aluminium Company and Bistral, d. o. o., from Slovenska Bistrica under contract No. 2410-0206-09.